J|A|C|S
ARTICLES

Published on Web 06/17/2009

Characterization of Dispersed Heteropoly Acid on Mesoporous Zeolite Using Solid-State ^{31}P NMR Spin−Lattice Relaxation

Kake Zhu, Jianzhi Hu, Xiaoyan She, Jun Liu,* Zimin Nie, Yong Wang, Charles H. F. Peden, and Ja Hun Kwak

Pacific Northwest National Laboratory, Richland, Washington 99352

Received February 19, 2009; E-mail: jun.liu@pnl.gov

Abstract: Dispersion and quantitative characterization of supported catalysts is a grand challenge in catalytic science. In this paper, heteropoly acid $H_3PW_{12}O_{40}$ (HPA) is dispersed on mesoporous zeolite silicalite-1 derived from hydrothermal synthesis using carbon black nanoparticle templates, and the catalytic activity is studied for 1-butene isomerization. The HPAs supported on conventional zeolite and on mesoporous zeolite exhibit very different activities and thus provide good model systems to investigate the structure dependence of the catalytic properties. The HPA on mesoporous silicalite-1 shows enhanced catalytic activity for 1-butene isomerization, while HPA on conventional silicalite-1 exhibits low activity. To elucidate the structural difference, supported HPA catalysts are characterized using a variety of techniques, including ^{31}P magic angle spinning nuclear magnetic resonance, and are shown to contain a range of species on both mesoporous and conventional zeolites. However, contrary to studies reported in the literature, conventional NMR techniques and chemical shifts alone do not provide sufficient information to distinguish the dispersed and aggregated surface species. The dispersed phase and the nondispersed phase can only be unambiguously and quantitatively characterized using spin−lattice relaxation NMR techniques. The HPA supported on mesoporous zeolite contains a fast relaxation component related to the dispersed catalyst, giving a much higher activity, while the HPA supported on conventional zeolite has essentially only the slow relaxation component with very low activity. The results obtained from this work demonstrate that the combination of spinning sideband fitting and spin−lattice relaxation techniques can provide detailed structural information on not only the Keggin structure for HPA but also the degree of dispersion on the support.

Introduction

Polyoxometalates (POMs) are a class of compounds formed from negatively charged inorganic metal−oxygen building blocks. When charge-balanced with cationic species, POMs self-assemble into unusual three-dimensional structures with specific topological and electronic properties.[1,2] POMs are commonly formed from polyanions of early transition metals such as W, Mo, or V. These anions can be substituted with other transition metals. The diversities in POMs' composition and structure make them attractive for many applications, particularly as Brønsted acid and redox catalysts. For example, POMs exhibit catalytic activity in olefin oxidation to epoxides, oxidative dehydrogenation of alkanes, or isomerization due to their redox and acidic properties. Both homogeneous and heterogeneous catalyses have been investigated.[3−7] However, POMs themselves are usually nonporous solids with surface area less than 10 m^2/g, and therefore they have limited surface sites for surface catalyzed reactions. To increase the surface accessibility, POMs are supported on high surface area weak-acidic or nonbasic supports,[6,8−12] complexed with large cations to create porosity between anions,[13−15] or immobilized on positively charged nanoparticles through electrostatic attraction[16,17] or ion-exchange between protons and metal cations.[18,19] Supported POMs not

(1) Pope, M. T.; Muller, A. *Angew. Chem., Int. Ed. Engl.* **1991**, *30*, 34–48.
(2) Pope, M. T. *Heteropoly and Isopoly Oxometalates*; Springer-Verlag: Berlin, 1983.
(3) Mizuno, N.; Misono, M. *Chem. Rev.* **1998**, *98*, 199–217.
(4) Neumann, R. Polyoxometalate complexes in organic oxidation chemistry. In *Progress in Inorganic Chemistry*; John Wiley & Sons Inc: New York, 1998; Vol. 47, p 317.
(5) Hill, C. L.; Prossermccartha, C. M. *Coord. Chem. Rev.* **1995**, *143*, 407–455.
(6) Chen, L. F.; Zhu, K.; Bi, L. H.; Suchopar, A.; Reicke, M.; Mathys, G.; Jaensch, H.; Kortz, U.; Richards, R. M. *Inorg. Chem.* **2007**, *46*, 8457–8459.
(7) Kozhevnikov, I. V. *Chem. Rev.* **1998**, *98*, 171–198.
(8) Khenkin, A. M.; Neumann, R.; Sorokin, A. B.; Tuel, A. *Catal. Lett.* **1999**, *63*, 189–192.
(9) Zhou, M.; Guo, L. P.; Lin, F. Y.; Liu, H. X. *Anal. Chim. Acta* **2007**, *587*, 124–131.
(10) Maksimchuk, N. V.; Meigunov, M. S.; Chesalov, Y. A.; Mrowlec-Bialon, J.; Jarzebski, A. B.; Kholdeeva, O. A. *J. Catal.* **2007**, *246*, 241–248.
(11) Kozhevnikov, I. V.; Sinnema, A.; Jansen, R. J. J.; Pamin, K.; Vanbekkum, H. *Catal. Lett.* **1995**, *30*, 241–252.
(12) Marme, F.; Coudurier, G.; Vedrine, J. C. *Microporous Mesoporous Mater.* **1998**, *22*, 151–163.
(13) Uchida, S.; Hashimoto, M.; Mizuno, N. *Angew. Chem., Int. Ed.* **2002**, *41*, 2814–2817.
(14) Uchida, S.; Mizuno, N. *Chem.—Eur. J.* **2003**, *9*, 5850–5857.
(15) Liu, Y. Y.; Koyano, G.; Na, K.; Misono, M. *Appl. Catal. A-Gen.* **1998**, *166*, L263−L265.

only improve accessibility for substrates but also, in some cases, enhance their catalytic activity through support interactions.[6,12−17]

Mesoporous silica has been used to support POMs because SiO_2 is chemically inert to the POM structures.[18−21] In most studies on supported POMs, the surface species and acidity are difficult to characterize and quantify because of the lack of solid-state techniques to unambiguously identify the surface species. Conventional techniques, such as titration with Hammett indicators and temperature-programmed desorption (TPD) of ammonia or pyridine, as well as adsorption microcalorimetry (using ammonia), have been used to study surface acidity.[20,21] However, since polar molecules are absorbed in bulk POM structures by forming the so-called "pseudo-liquid" phases, the conventional techniques cannot be easily used to differentiate the dispersed and nondispersed POMs.[3,20,21] Probe reactions using nonpolar substrates give only indirect evidence of surface acidity. Other techniques, such as ^{31}P or ^{29}Si MAS NMR, are frequently used to study supported POMs by assigning different resonance peaks in the NMR spectra to different species. On amorphous silica surfaces, two species have been identified for Keggin heteropoly acid $H_3PW_{12}O_{40}$ (HPA) structure. One is around 15 ppm from intact HPA, and another one around −14 ppm is attributed to $H_2P_6W_{18}O_{62}$ (−13.0 ppm) or $H_6P_2W_{21}O_{71}$ (−13.5 ppm).[22] Lefebvre has suggested the existence of deprotonated $(SiOH_2^+)(H_2PW_{12}O_{40}^-)$ at −14.6 ppm.[23] Spin−lattice relaxation has been employed to detect the surface structure of POMs with Keggin[24,25] and Dawson structures[26] by Thouvenot and co-workers, who have found that surface coverage of POMs on silica increases with loading and is a function of spin−lattice relaxation time of the heteroatoms such as ^{31}P or ^{29}Si. However, only a mean relaxation time T_1 is deduced, and the surface species and their relationship with catalytic activity are not reported. In general, it is difficult to clearly delineate the states of surface species and their relationship with catalytic activities using the above-mentioned techniques.

In this paper, we report the use of mesoporous zeolite as a support for Keggin-type HPA. The catalytic activity is studied for 1-butene isomerization. By comparing the activities on the different supports and combining the NMR results, we demonstrate that the HPA Keggin structure, the dispersed species, and the agglomerated species can be unambiguously identified and quantified through ^{31}P NMR spin−lattice relaxation and ^{31}P chemical shift anisotropy from fitting of spinning sideband (SSB). The techniques of NMR characterizations and structural information we draw from this study provide new insights into supported POMs.

Zeolites with mesoporosity have been developed by Jacobsen and co-workers to circumvent the pore-size limitation of microporosity using carbon black as a hard template to create additional porosity during the crystallization process.[27] A variety of hard templates and leaching methods have been developed to prepare zeolites with mesostructures.[27−32] Mesoporous zeolites have shown improved catalytic activities compared to conventional zeolites or amorphous silica with mesopores as a result of enhanced porosity and crystalline nature of the support.[29,33−35] Metals, alloys, and carbides can be readily dispersed into the mesopores of the zeolites, while it is more challenging to disperse these clusters in conventional zeolites. Dispersion of these clusters on conventional zeolites often results in large aggregates deposited on the outer surface of zeolitic crystals, due to the hindrance imposed by micropores.[36]

Conventional and mesoporous silicalite-1 are used as catalyst supports in this study. These materials by themselves have no catalytic activity for 1-butene isomerization. The mesoporosity is created by using carbon black templates during zeolite synthesis, and HPA is loaded into the support by impregnation using a rotary evaporation technique. HPA with a well-known Keggin structure is selected as a model HPA. The size of primary HPA structure is 1.2 nm, larger than the dimension of most conventional zeolites channels. Our results show that HPA can access the mesopores and be deposited on the internal surface with preserved Keggin structure to give higher catalytic activity toward the isomerization of 1-butene as compared to HPA supported on conventional silicalite-1.

Experimental Section

Synthesis. Meso-silicalite-1 was prepared using the method reported by Jacobsen.[27] Black Pearls 2000 carbon black from Cabot Corp. was used as templates to create mesoporosities. Tetraethoxysilane and tetrapropylammonium hydroxide (40 wt % aqueous solution) were purchased from Alfa Aesar, and anhydrous ethanol was from Aldrich. All the purchased chemicals were used without further purification. The as-prepared carbon−zeolite composite was calcined in a muffle oven at 550 °C for 5 h to remove the carbon black and the organic templates. To prepare HPA/meso-silicalite-1, 0.2 g of $H_3PW_{12}O_{40}\cdot nH_2O$ (Aldrich) was dissolved in 10 mL of ethanol, 0.5 g of meso-silicalite-1 was dispersed in the solution, and the mixture was dried by rotary vacuum evaporation at 60 °C. The sample was further baked in an oven at 120 °C overnight. The same procedure was used to deposit HPA on pure silicalite-1 without mesoporosity, which was purchased from Aldrich. HPA loading was ca. 28.6 wt % for both samples.

Activity Measurement. The catalytic activity measurements for 1-butene isomerization were carried out with a quartz flow fixed-

(16) Okun, N. M.; Anderson, T. M.; Hill, C. L. *J. Am. Chem. Soc.* **2003**, *125*, 3194–3195.
(17) Okun, N. M.; Anderson, T. M.; Hill, C. L. *J. Mol. Catal. A-Chem.* **2003**, *197*, 283–290.
(18) Wang, Y.; Peden, C. H. F.; Choi, S. *Catal. Lett.* **2001**, *75*, 169–173.
(19) Soled, S.; Miseo, S.; McVicker, G.; Gates, W. E.; Gutierrez, A.; Paes, J. *Catal. Today* **1997**, *36*, 441–450.
(20) Farneth, W. E.; Gorte, R. J. *Chem. Rev.* **1995**, *95*, 615–635.
(21) Bardin, B. B.; Bordawekar, S. V.; Neurock, M.; Davis, R. J. *J. Phys. Chem. B* **1998**, *102*, 10817–10825.
(22) Kozhevnikov, I. V.; Kloetstra, K. R.; Sinnema, A.; Zandbergen, H. W.; vanBekkum, H. *J. Mol. Catal. A-Chem.* **1996**, *114*, 287–298.
(23) Lefebvre, F. *J. Chem. Soc., Chem. Commun.* **1992**, 756–757.
(24) Thouvenot, R.; Fournier, M.; Rocchicciolideltcheff, C. *J. Chem. Soc., Faraday Trans.* **1991**, *87*, 2829–2835.
(25) Thouvenot, R.; Rocchicciolideltcheff, C.; Fournier, M. *J. Chem. Soc., Chem. Commun.* **1991**, 1352–1354.
(26) Contant, R.; Rocchicciolideltcheff, C.; Fournier, M.; Thouvenot, R. *Colloids Surf. A: Phys. Chem. Eng. Aspects* **1993**, 301–306.
(27) Jacobsen, C. J. H.; Madsen, C.; Houzvicka, J.; Schmidt, I.; Carlsson, A. *J. Am. Chem. Soc.* **2000**, *122*, 7116–7117.
(28) Egeblad, K.; Christensen, C. H.; Kustova, M.; Christensen, C. H. *Chem. Mater.* **2008**, *20*, 946–960.
(29) Tao, Y. S.; Kanoh, H.; Abrams, L.; Kaneko, K. *Chem. Rev.* **2006**, *106*, 896–910.
(30) Zhu, K.; Egeblad, K.; Christensen, C. H. *Eur. J. Inorg. Chem.* **2007**, *395*, 5–3960.
(31) Cejka, J.; Mintova, S. *Catal. Rev.* **2007**, *49*, 457–509.
(32) Perez-Ramirez, J.; Christensen, C. H.; Egeblad, K.; Groen, J. C. *Chem. Soc. Rev.* **2008**, *37*, 2530–2542.
(33) Christensen, C. H.; Johannsen, K.; Schmidt, I.; Christensen, C. H. *J. Am. Chem. Soc.* **2003**, *125*, 13370–13371.
(34) Xiao, F. S.; Wang, L. F.; Yin, C. Y.; Lin, K. F.; Di, Y.; Li, J. X.; Xu, R. R.; Su, D. S.; Schlogl, R.; Yokoi, T.; Tatsumi, T. *Angew. Chem., Int. Ed.* **2006**, *45*, 3090–3093.
(35) Choi, M.; Cho, H. S.; Srivastava, R.; Venkatesan, C.; Choi, D. H.; Ryoo, R. *Nat. Mater.* **2006**, *5*, 718–723.
(36) Christensen, C. H.; Schmidt, I.; Carlsson, A.; Johannsen, K.; Herbst, K. *J. Am. Chem. Soc.* **2005**, *127*, 8098–8102.

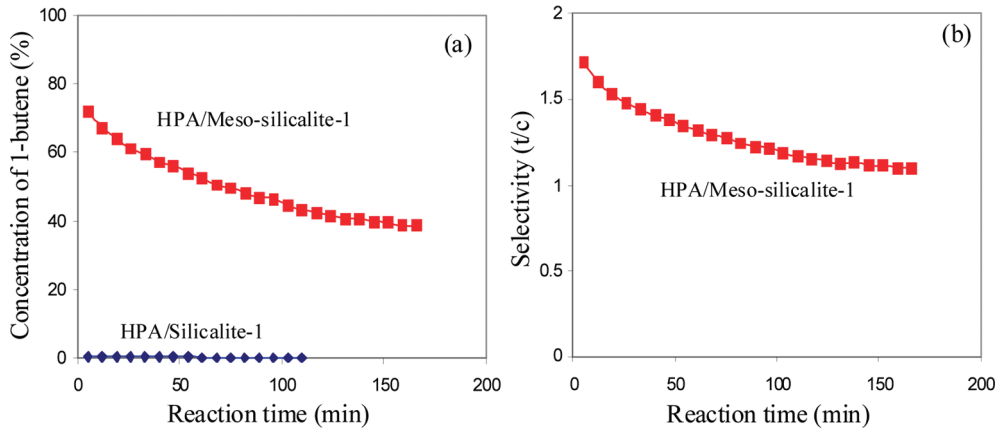

Figure 1. Conversion (a) and trans/cis ratio (b) for isomerization of 1-butene over HPA/meso-silicalite-1 and HPA/silicalite-1 as a function of time on stream. The trans/cis ratio for HPA/silicalite-1 is not shown because the product yields are too low to determine.

bed reactor (1 cm i.d.) at atmospheric pressure. Typically, 20 mg of sample (pelletized, 60−100 mesh) was loaded onto the quartz frit. The catalyst was first pretreated in helium at 200 °C for 1 h, and then the isomerization reaction was performed at 70 °C. The feed gas contained 0.5% 1-butene and was flowed at 50 mL/min. The gas effluent from the reactor was analyzed by a gas chromatograph (HP 5890) equipped with a HAYESEP T column and flame ionization and thermal conductivity detectors.

Characterizations. The X-ray diffraction (XRD) patterns in $\theta-2\theta$ scan mode were obtained on a Philips Xpert X-ray diffractometer using Cu Kα radiation at $\lambda = 1.54$ Å. Nitrogen adsorption data were collected using a Quantachrome autosorb-6 automated gas sorption system. Prior to physisorption measurements, all samples were outgassed under vacuum at 80 °C overnight. Total surface areas were calculated according to the BET method. Micropore volumes were calculated by the *t*-plot method. Total pore volumes were estimated from the amount of N_2 adsorbed at $p/p_0 = 0.99$. Meso-/macropore volumes were calculated by subtracting micropore volumes from total pore volumes. Barret−Joyner−Halenda (BJH) calculation was employed to estimate the pore-size distribution for the mesoporous samples. Scanning electronic microscopy (SEM) was conducted on a JEOL JSM-5900LV instrument at 20 kV. Transmission electron microscopy (TEM) studies were conducted on a JEOL JEM 2010 microscope at 200 kV.

^{31}P magic angle spinning nuclear magnetic resonance (MAS NMR) experiments were performed on a Varian-Chemagnetics 300 MHz Infinity spectrometer, corresponding to ^{1}H and ^{31}P Larmor frequencies of 299.982 and 121.43 MHz, respectively. A commercial MAS probe with a 7.5 mm outside diameter and 6 mm internal diameter pencil-type spinner system was used. The sample cell resembled the commercial cell except that two solid Teflon plugs were made in such a manner that they could only be fully inserted into the zirconium cylinder after precooling using liquid nitrogen to seal ~200 mg (HPA), 76 mg (HPA/silicalite-1), and 73 mg (HPA/meso-silicalite-1) samples for ^{31}P MAS NMR studies. Since HPA and HPA-supported catalysts are sensitive to the degree of hydration, sealing the samples reduces dehydration during the MAS NMR experiments. The chemical shifts were referenced to 80% H_3PO_4 (0 ppm). All spectra were acquired at room temperature with high-power ^{1}H decoupling applied during data acquisition to samples after catalytic tests.

Results and Discussion

Catalytic activities of HPA/silicalite-1 and HPA/meso-silicalite-1 are evaluated for isomerization of 1-butene at 70 °C. Figure 1 shows 1-butene conversion and trans/cis ratio as a function of time on stream. A much higher activity is observed over HPA/meso-silicalite-1 than over HPA/silicalite-1. For example, the initial conversion of 1-butene is 72% on HPA/meso-silicalite-1 with a *trans*- to *cis*-2-butene ratio of around 1.7, while conversion for HPA/silicalite-1 is less than 1%. The conversion decreases with time on stream over 180 min, possibly due to coke formation which blocks some of the active proton sites, a phenomenon generally observed on solid acid catalysts.[37] The catalytic activity of double bond shift is driven by Brønsted acidic sites from HPA, which in turn is governed by the structure of HPAs on the support. Since HPA/silicalite-1 has the species of low catalytic activity while HPA/meso-silicalite-1 has the species with high activity, these two samples serve as good model systems to discriminate the aggregated and dispersed species of HPA and will provide new information on structure−activity relationships.

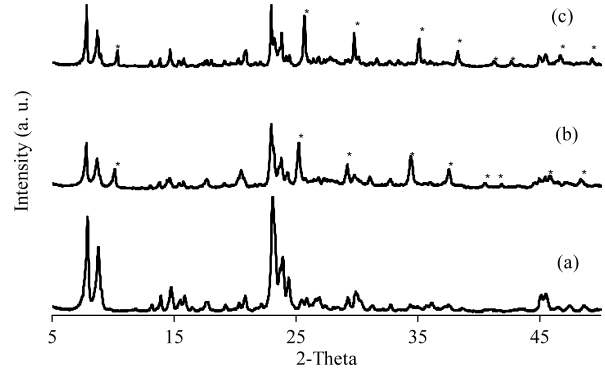

Figure 2. X-ray diffraction patterns of meso-silicalite-1 (a), HPA/meso-silicalite-1 (b), and HPA/silicalite-1 (c), where the peaks with stars correspond to JCPDS No. 75-2152 of Keggin-type $H_3PW_{12}O_{40}$. All the rest of the peaks belong to JCPDS No. 89-1421 of MFI-structured silicalite-1.

XRD patterns of the two samples are shown in Figure 2. The pure silicalite-1 and meso-silicalite-1 possess typical peaks from MFI-structured (JCPDS No. 89-1421) silicalite-1 without any other crystalline phases.[38] After loading with HPA, the XRD patterns of both conventional silicalite-1 and meso-silicalite-1 show another series of peaks which belong to HPA (JCPDS No. 75-2152) besides the peaks from silicalite-1. These results show that some HPA presents as crystalline phase due to surface aggregation. The XRD peaks from HPA on meso-silicalite-1

(37) Bardin, B. B.; Davis, R. J. *Appl. Catal. A-Gen.* **2000**, *200*, 219–231.
(38) Kokotailo, G. T.; Lawton, S. L.; Olson, D. H.; Olson, D. H.; Meier, W. M. *Nature* **1978**, *272*, 437–438.

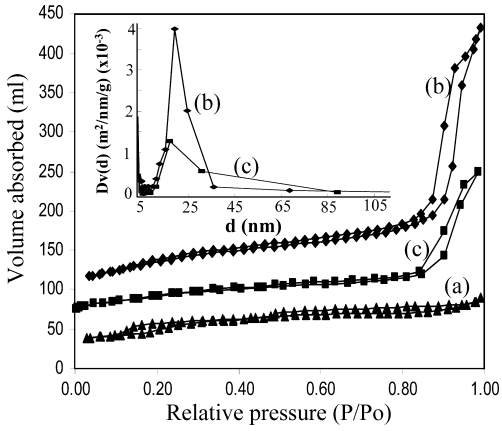

Figure 3. Nitrogen adsorption of HPA/silicalite-1 (a), meso-silicalite-1 (b), and HPA/meso-silicalite-1 (c). The inset shows the corresponding pore size distributions. The volume of adsorption is shifted vertically for clarity.

are broader than those supported on silicalite-1, suggesting reduced particle sizes on the mesoporous zeolite support. Careful examination of the XRD patterns also reveals that HPA peaks on mesoporous zeolite and on conventional zeolite are slightly shifted. Such a shift may be a result of different degrees of crystallization and interactions with the substrates, as Keggin structures change *d*-spacing with environment.[39] Conventional XRD measures long-range ordered crystalline structures qualitatively, and noncrystalline HPA cannot be identified.

N_2 adsorption−desorption patterns are shown in Figure 3. For HPA/silicalite-1, the isotherm shows that only micropores exist in the solids. Additionally, two very small "hysteresis loops" can be identified, which are sometimes misunderstood in terms of additional porosity. The first loop appears between relative pressures of 0.1 and 0.2 due to the fluid-to-crystalline phase transition of nitrogen in the silicalite-1 channels, which delays the pressure to higher values and is a unique phenomenon of MFI-type zeolite with high Si/Al ratios.[40−42] Another loop at 0.41−0.48 is from the tensile strength effect, driven from liquid nitrogen itself, and does not suggest the existence of additional porosity.[40] For meso-silicalite-1 and HPA/meso-silicalite-1, the isotherms belong to type IV adsorption of IUPAC classifications with an obvious type H1 hysteresis loop starting at relative pressure >0.8, suggesting the existence of mesopores before and after HPA loading. The fluid-to-crystalline phase transition and the tensile strength effect are usually not obvious for mesoporous silicalite-1. The analytical data for surface area and porosity are listed in Table 1. The surface area decreases after HPA loading. As HPA has a high density and its loading increases the density of the composite, the specific surface area and pore volume decrease. The BJH method is used to estimate the mesopore size distribution of meso-silicalite-1 with and without HPA. The corresponding decrease of mesopore volume is also manifested in Figure 3 (inset) and Table 1. It is seen that pore size distribution is wide, as the carbon black template has a wide distribution of particle diameters. The average pore size decreases from 19 to 17 nm after HPA is loaded, suggesting that HPA partially fills the mesopores.

(39) Pizzio, L. R.; Blanco, M. N. *Appl. Catal. A-Gen.* **2003**, *255*, 265–277.
(40) Groen, J. C.; Peffer, L. A. A.; Perez-Ramirez, J. *Microporous Mesoporous Mater.* **2003**, *60*, 1–17.
(41) Llewellyn, P. L.; Coulomb, J. P.; Grillet, Y.; Patarin, J.; Andre, G.; Rouquerol, J. *Langmuir* **1993**, *9*, 1852–1856.
(42) Llewellyn, P. L.; Coulomb, J. P.; Grillet, Y.; Patarin, J.; Lauter, H.; Reichert, H.; Rouquerol, J. *Langmuir* **1993**, *9*, 1846–1851.

Table 1. N_2 Adsorption−Desorption Analyses of Meso-silicalite-1, HPA/Meso-silicalite-1, and HPA/Silicalite-1

sample	BET surface area (m^2/g)	macro- + mesopore volume[a] (mL/g)	mesopore size[b] (nm)	micropore volume (mL/g)
HPA/silicalite-1	266			0.03
meso-silicalite-1	418	0.56	19	0.11
HPA/meso-silicalite-1	285	0.31	17	0.08

[a] Macro- + mesopore volume is calculated by subtraction of total pore volume at relative pressure of 0.99 from micropore volume by the *t*-plot method. [b] Mesopore diameter is estimated from BJH method using the desorption curve of the corresponding isotherms.

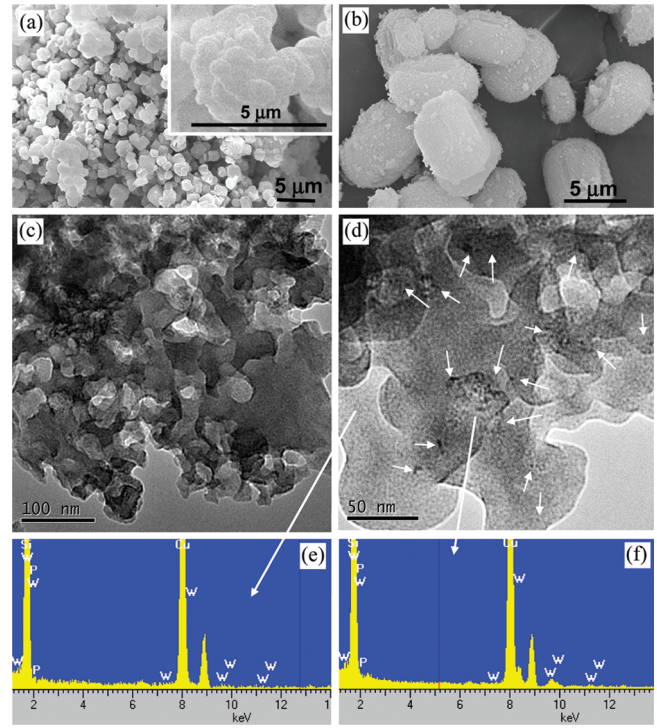

Figure 4. SEM and TEM images of supported HPA. (a) SEM image of HPA/silicalite-1. The inset shows the precipitated HPA outside the silicalite-1 crystals. (b) SEM image of HPA/meso-silicalite-1. (c) TEM image of the meso structure in HPA/meso-silicalite-1. (d) High-magnification TEM image of HPA/meso-silicalite-1. The dark particles indicated by the arrows are HPA. (e) EDS spectrum from the meso-silicalite-1 substrate. (f) EDS spectrum from the region containing HPA.

SEM images of HPA/silicalite-1 and HPA/meso-silicalite-1 are shown in Figure 4a,b. Well-crystallized, microsized rectangular particles are observed in both panels. For the conventional silicalite-1, many "amorphous"-looking particles are observed on top of the regular rectangular crystals (inset) due to the precipitation and deposition HPA particles outside the zeolite crystals. For meso-silicalite-1-supported HPAs, the zeolite particles are mostly separated. Very small HPA particles are also observed on the rectangular particle surface, suggesting that the HPA particles are deposited both inside and outside the crystals. To investigate the distribution and structure of HPA/meso-silicalite-1, TEM images are obtained from thin sectioned (0.1 μm) samples (Figure 4c,d). Continuous 20−50 nm mesoporous channels can be clearly observed. In addition, dark spots can be observed on the pore surface, as indicated by arrows. The W edge is revealed in energy dispersive spectroscopy (EDS) spectra, but the P peaks cannot be isolated from the Si edge. The TEM study provides good evidence of

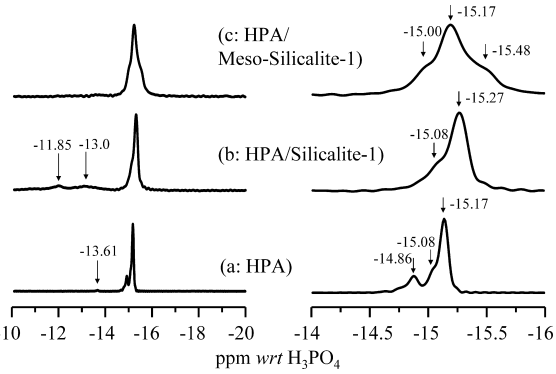

Figure 5. ^{31}P MAS NMR spectra acquired at a sample spinning rate of 5 kHz: (a) HPA, (b) HPA/silicalite-1, and (c) HPA/meso-silicalite-1. Left traces are full spectra while right traces are horizontally expanded between −14 and −16 ppm. All the spectra are acquired using a recycle delay time of 5 s with the number of accumulations 60 (a), 48 020 (b), and 3108 (c), respectively.

typical mesoporous structure of the silicalite-1 and shows that HPA particles are deposited in the mesoporous channels.

To further elucidate the structure of HPA upon loading, the ^{31}P MAS NMR technique is used. Figure 5 shows the ^{31}P MAS NMR spectra of HPA (a), HPA/silicalite-1 (b), and HPA/meso-silicalite-1 (c) acquired at a sample spinning rate of 5 kHz. For HPA, the line width ($\Delta\upsilon_{1/2}$) obtained from line shape deconvolution, defined as the line width at the half peak height positions of the most intense peak (the peak at −15.17 ppm), in Figure 5a is about 8.5 Hz, or 0.07 ppm. Such a high spectral resolution allows fine features to be observed in HPA, including a low-intensity shoulder peak at about −15.08 ppm ($\Delta\upsilon_{1/2}$ = 9.3 Hz), a minor peak at −14.86 ppm ($\Delta\upsilon_{1/2}$ = 10.17 Hz), and a minor sharp peak with $\Delta\upsilon_{1/2}$ = ∼9.6 Hz at −13.61 ppm due to dehydration. Note that the integrated spectral intensity for the −13.61 ppm peak accounts for only about 1% of the total spectral intensity, while the major peak centered at −15.17 ppm has about 71% of the total spectral intensity. The peak at −15.17 ppm is thus assigned to crystalline HPA molecules having long-range orders. It is known that the ^{31}P MAS NMR peaks corresponding to different hydration states of HPA molecules vary between −11.1 and −15.6 ppm.[43] Since the −14.86 ppm (15%) and the −15.04 ppm (13%) peaks are very close to the −15.17 ppm, these two peaks can be assigned to crystalline HPA molecules that have hydration states slightly different from that of the molecules associated with the −15.17 ppm peak.

For the HPA/silicalite-1 sample, a major peak at −15.27 ppm with $\Delta\upsilon_{1/2}$ = ∼20 Hz (relative ratio is 81.6% if only the chemical shift range from −14 to −16 ppm is considered) is observed. A shoulder peak centered at about −15.08 ppm with $\Delta\upsilon_{1/2}$ = ∼24 Hz (18.4% if only the chemical shift range from −14 to −16 ppm is considered) is also observed. This shoulder peak is at exactly the same location as the corresponding shoulder peak for HPA (Figure 5b). The overall integrated spectral intensity for these two peaks is about 74% of the overall spectral intensity. Two other low-intensity peaks are observed at −11.85 ($\Delta\upsilon_{1/2}$ = ∼80 Hz) and −13.0 ppm ($\Delta\upsilon_{1/2}$ = ∼150 Hz), respectively. On the basis of the chemical shifts and the significantly increased line width, we hypothesize that these two low-intensity peaks correspond to HPA molecules that are at a low dehydration state or HPA molecules with some structural distortions due to dehydration.[43] As high silicon MFI-structured zeolites are hydrophobic, dehydration may occur at the interfaces. The increased line width associated with the major peak at −15.27 ppm (20 Hz) relative to that (8.5 Hz) of the −15.17 ppm major peak in Figure 5a indicates that the particle size is reduced, i.e., long-range order decreases. The major peak (−15.27 ppm) is upfield-shifted by 0.1 ppm compared with the −15.17 ppm peak in HPA, suggesting a slightly increased shielding (increased electronic cloud around the phosphorus nucleus), possibly due to a combination of reduced particle size and the interaction of particles with the silicalite-1 surfaces.

For the ^{31}P MAS NMR spectrum of the HPA/meso-silicalite-1 sample in Figure 5c, only three peaks are observed, including a major peak at −15.17 ppm and two shoulder peaks at about −15.0 and −15.48 ppm. There is no peak observed from −11 to −14 ppm. The fact that all the peaks are centered at around −15 ppm suggests that the basic structure of HPA molecules is preserved in the HPA/meso-silicalite-1 sample. The spectrum in Figure 5c can be fit with three Lorentz line shapes with peaks (line width, relative integrated ratio) at −14.96 ppm ($\Delta\upsilon_{1/2}$ = ∼20 Hz, 7%), −15.196 ppm (31.9 Hz, 73.4%), and −15.46 ppm (32.8 Hz, 19.6%), respectively. Compared with the line width of the major peaks (20−24 Hz) obtained from Figure 5b for the HPA/silicalite-1 sample, the line width for the dominant peaks (∼32 Hz) in HPA/meso-silicalite-1 is further broadened, indicating that the particle size is further decreased. Both the increased line width and the appearance of a new peak at −15.48 ppm suggest different environments for the HPA species in meso-silicalite-1, but the exact nature of these species cannot be identified from such NMR spectra.

Figure 6a−c illustrates the ^{31}P spectra as a function of the recovery time at several selected recovery times between 3 and 150 s. The spin−lattice relaxation times (T_1) are measured for the resonance as an average using the standard saturation-recovery method, and the results are summarized in Figure 6d. A single T_1 is found for both the HPA and the HPA/silicalite-1 sample with T_1 = 24 s for HPA and T_1 = 67 s for HPA/silicalite-1. However, the relaxation data for HPA/meso-silicalite-1 cannot be fit using a single exponential function (Figure 6e). Rather the data can only be fit using two exponential functions with distinct relaxation times, i.e., a fast-relaxing component (T_{1f}) and a slow-relaxing component (T_{1s}). The fast-relaxing component hasT_{1f} = 2.7 s with a relative abundance ratio of 46%, while the slow-relaxing component has T_{1s} = 64 s with a relative abundance ratio of 54%. It is important to note that T_{1s} (64 s) of the slow-relaxing component is almost the same as that (67 s) found in the HPA/silicalite-1 sample. This coincidence indicates that both silicalite-1 and meso-silicalite-1 have the same slow-relaxing component, while the fast-relaxing component (T_{1f} = 2.7 s) only exists on meso-silicalite-1. In solid-state NMR, because of the restricted freedom of motion, increased molecular/segmental motion often means a short T_1 value.[44] Since the fast relaxation time is related to increased freedom of motion due to small cluster sizes or HPA interacting with surface silanols by means of proton transfer to form $-OH_2^+(H_2PW_{12}O_{40})^-$, we suggest that the fast relaxation component is associated with the well-dispersed HPA catalytic species on meso-silicalite-1. Since the relaxation time T_1 actually differentiates the dispersed and nondispersed HPAs, this method can be used to quantify the dispersed HPAs from bulk HPAs. Compared with TPD or microcalorimetry methods using a base

(43) Kanda, Y.; Lee, K. Y.; Nakata, S.; Asaoka, S.; Misono, M. *Chem. Lett.* **1988**, 139–142.

(44) Slichter, C. P. *Principles of Magnetic Resonance*; Springer-Verlag: Berlin, 1990.

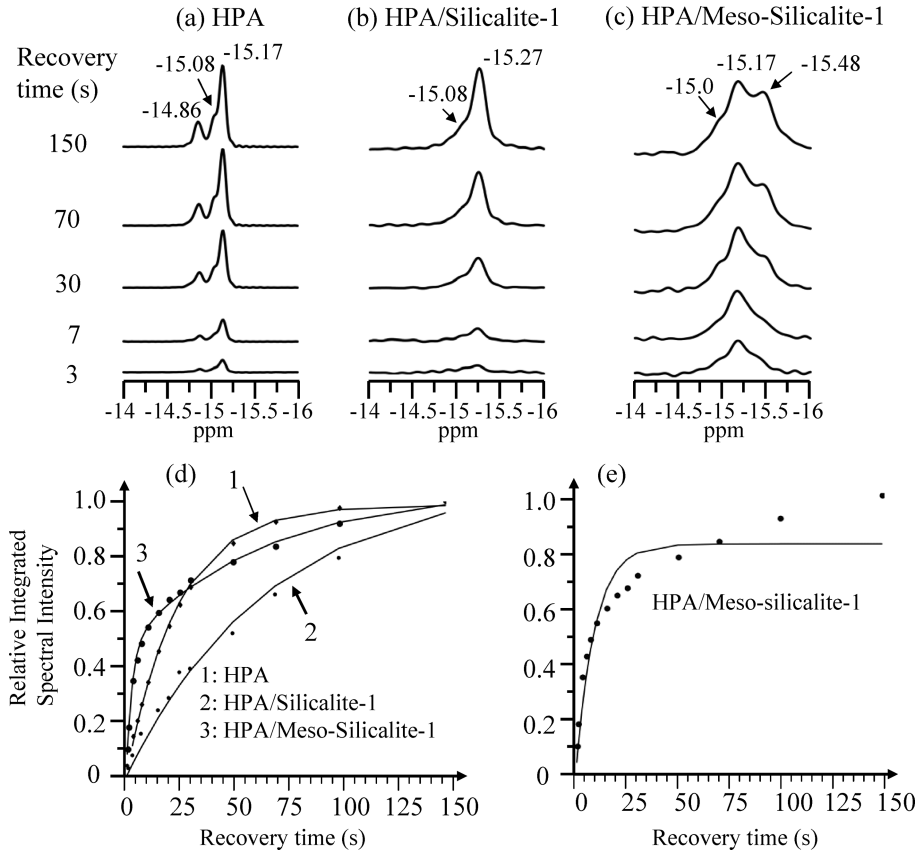

Figure 6. Spin−lattice relaxation NMR spectra. (a−c) ^{31}P MAS NMR spectra of meso-silicate-1 sample as a function of several selected recovery times. The spectra are acquired at a sample spinning rate of 5 kHz. The accumulation number used for acquiring each spectrum is 256. (a) HPA, (b) HPA/silicalite-1, and (c) HPA/meso-silicalite-1. (d) The integrated ^{31}P MAS NMR spectral intensity from −14 to −16 ppm as a function of the saturation recovery time for HPA (1), $T_1 = 24.4$ s (100%); HPA/silicalite-1 (2), $T_1 = 67.7$ s (100%); and HPA/meso-silicalite-1 (3), $T_{1f} = 2.7$ s (46%), $T_{1s} = 63.7$ s (54%) (double exponential fitting), respectively. Note that both (1) and (2) are fit using a single exponential rise function, while (3) can only be fit using double exponential rise functions. (e) Result for single exponential fitting of HPA/meso-silicalite-1.

probe molecule that can be absorbed into the bulk HPA structure, the T_1 method offers unambiguous determination of the dispersed phase. Furthermore, the TPD method estimates the total number of adsorbed/absorbed sites from integrated peak intensity of varied temperatures but does not provide information of the Keggin structure and surface properties at the specific reaction temperature. The ability of the spin−lattice relaxation to discriminate the dispersed HPAs from bulk phase will be valuable in understanding the relationship between catalytic activity and HPA structure.

Furthermore, we demonstrate that the surface species are quite complex and cannot be adequately characterized by chemical shifts alone. For example, for the HPA/meso-silicalite-1, the intensity of the shoulder peak centered at −15.48 ppm increases significantly at a recovery time of 150 s, while below 30 s this peak has relatively low intensity. This result indicates that the sharp peak at −15.48 ppm has a rather long relaxation time. By dividing each spectrum into three spectral ranges, −14.68 to −15.0 ppm, −15.0 to −15.33 ppm, and −15.33 to −15.95 ppm, we have found that for each spectral range the relaxation data can only be fit with double exponential functions consisting of a fast and a slow relaxation component. This result unambiguously indicates that the fast relaxation component has broad spectral line features ranging from −14.68 to −15.96 ppm, which are severely overlapped with the three relative sharp spectral features centered at −15.0, −15.17, and −15.48 ppm. If we take the half line width for the fast-relaxing component from −14.68 to −15.96 ppm, the value in hertz would be 155. This result strongly supports our hypothesis that the line width corresponding to the dispersed HPA would be much larger compared to that (<31 Hz) of the HPA agglomerates.

Finally, to validate the basic structural integrity of dispersed HPA molecules, we have carried out ^{31}P MAS NMR experiments at a slow spinning rate of 200 ± 1 Hz. The results are summarized in Figure 7. The principal values (δ_{11}, δ_{22}, δ_{33}) of ^{31}P chemical shift anisotropy are determined by fitting the SSB pattern corresponding to the isotropic chemical shift range between −14.68 and −15.96 ppm with a single tensor using the Herzfeld−Berger method.[45] Note that the integrated spectral intensity for each SSB is used for the simulation. The resulting principal values are ($\delta_{11} = -13.3$, $\delta_{22} = -15.61$, $\delta_{33} = -16.47$ ppm) for HPA, ($\delta_{11} = -11.85$, $\delta_{22} = -15.48$, $\delta_{33} = -18.48$ ppm) for HPA/silicalite-1, and ($\delta_{11} = -12.17$, $\delta_{22} = -15.2$, $\delta_{33} = -18.19$ ppm) for HPA/meso-silicalite-1. For the convenience of discussion, we define the anisotropy span as $\delta_{33} - \delta_{22}$. The very small anisotropy span, 3.16 ppm, for the HPA sample indicates that the phosphorus is located in a highly symmetrical electronic environment. The electronic cloud around the nucleus has nearly spherical symmetry. For the HPA/silicalite-1, the phosphorus symmetry is slightly perturbed, as evidenced by the increased intensities in SSBs. However, the deviation from the original bulk HPA molecules is small because the anisotropy span is only slightly increased to 6.6 ppm. Compared with bulk HPA, this slight change in anisotropy

(45) Herzfeld, J.; Berger, A. E. *J. Chem. Phys.* **1980**, *73*, 6021.

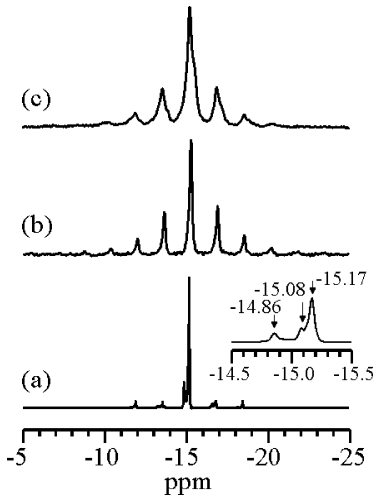

Figure 7. ^{31}P MAS NMR spectra acquired at a sample spinning rate of 200 ± 1 Hz: (a) HPA, (b) HPA/silicalite-1, and (c) HPA/meso-silicalite-1. All the spectra are acquired using a recycle-delay time of 5 s. The numbers of accumulations are 460 (a), 17 768 (b), and 30 064 (c), respectively.

span is no doubt due to the decreased particle size. On the basis of the long ^{31}P relaxation T_1, the reasonable narrow line width (<24 Hz), and the nearly zero isomerization reactivity, the HPA molecules in the HPA/silicalite-1 sample must be in an agglomerate state. The ^{31}P anisotropy span, i.e., 6.02 ppm, for the HPA/meso-silicalite-1 sample is very close to but slightly less than that (6.6 ppm) of the HPA/silicalite-1 sample. This result indicates that the basic HPA structure is still maintained in the HPA/meso-silicalite-1 sample.

Conclusions

In summary, we have found that Keggin-type $H_3PW_{12}O_{40}$ can enter the mesopores of hierarchically porous silicalite-1 by solvent evaporation, and the improved dispersion of HPA in large pores promotes catalytic activity for 1-butene isomerization. For HPA on conventional silicalite-1, the HPA resides mainly outside the crystalline microporous structure as crystalline agglomerates and is catalytically less active. It has been shown that the line width in the ^{31}P MAS NMR spectrum of HPA supported on a solid silicalite-1 surface is increased as the particle size is decreased. The well-dispersed HPA molecules give the largest line width. Furthermore, the ^{31}P spin−lattice relaxation time, T_1, corresponding to the well-dispersed HPA molecules is short, while the T_1 of HPA agglomerates is long. Our results indicate that, on the regular silicalite-1 surface, HPA molecules exist as small agglomerates, while on the meso-silicalite-1 surface, about 46% of the HPA molecules are successfully dispersed to the mesoporous channel surfaces. The structural integrity of the surface-exchanged HPA molecules is preserved. Coupled with reaction data, it can be concluded unambiguously that the well-dispersed HPA molecules are the active centers for isomerization of 1-butene.

Acknowledgment. The work is supported by the Laboratory-Directed Research and Development Program (LDRD) of the Pacific Northwest National Laboratory (PNNL) and by the Office of Basic Energy Sciences (BES), U.S. Department of Energy (DOE). TEM and NMR investigation was performed in the Environmental Molecular Sciences Laboratory, a national scientific user facility sponsored by the Department of Energy's Office of Biological and Environmental Research and located at Pacific Northwest National Laboratory. PNNL is a multiprogram laboratory operated by Battelle Memorial Institute for the Department of Energy under Contract DE-AC05-76RL01830.

JA901317R